What Causes Tides?

Yongfeng Yang
Bureau of Water Resources of Shandong Province
No. 127, Lishan Road, Jinan, Shandong Province, 250014, CHINA
e-mail: roufeng_yang@yahoo.com; roufengyang@gmail.com

Abstract
It has been known for thousands of years that the waters of coastal seas ebb and flow on a daily basis. This movement is long-term thought to be due to the gravitational pulls of the Moon and Sun. However, an in-depth investigation shows this understanding unreachable. Here we propose, the Earth's curved motions about the centre of mass of the Earth-Moon system and around the Sun create some centrifugal effects to stretch the Earth's body. Under the effect of the deformation, the rotating Earth drives its each part to regularly move up and down, this gives birth to some oscillations for ocean basins, generating water transferring, and also the rises and falls of water level regionally.

1 Introduction
1.1 A brief retrospect of tidal ideas

From antiquity it has been familiar that coastal seas always perform daily regular movements of water rise and fall. Since these movements are closely related to the frequently coastal activities, explaining them has undoubtedly tested human wisdom for millennia. Aristotle (384-322 BC) was highly perplexed and vaguely attributed it to the rocky nature of the coast. Early Chinese considered tides as the beating of the Earth's pulse and alternatively, it was believed to be caused by the Earth's breathing. Some people thought tides were caused by the different depths of ocean water. Galileo considered that the rotations of the Earth around the Sun and about its axis induced motions of the sea to generate the tides. However, the majority certainly linked tidal action to the influence of the Moon and of the Sun. Seleucus (lived in the 2nd century BC) was the first to consider this connection. He concluded the height of tide was correlated with the Moon's position relative to the Sun. However, the exact determination of how the Moon and Sun cause tides is unknown. A few Arabic explanations proposed that the Moon uses its rays to heat the water and then expand it. Descartes argued that space was full of ethereal substance and the resulting stresses between the ether and the Earth's surface gave birth to tides when the Moon travelled round the Earth. In contrast, Kepler and Newton represent those who expressly define this influence as the attraction of the Moon and Sun on the water. Newton formulated an attractive mechanism to account for the tide, within it the gravity gradient of the Moon produces a pair of bulges of water on Earth (that is in the line of the Earth-Moon system). As Newton and the well known 1740's Essayists (such as Daniel Bernoulli, Leonhard Euler, Colin Maclaurin, and Antoine Cavalleri, for instance) had assumed the oceans' response to the tidal driving force to be quasi-static, considering the complexity of actual oceans and currents, Laplace developed a set of hydrodynamic equations of continuity and momentum for a fluid on a rotating earth. Together with the following endeavors (including William Thomson, Baron Kelvin, Henri Poincaré, Arthur Thomas Doodson, etc.,), the idea of gravitation as the cause of tide (the attractive mechanism) was increasingly consolidated and became the cornerstone of modern tidal theories. A fuller review of the tidal history may be found in these works [1,2,3,4]. Undoubtedly, an accurate knowledge of tide involves in a variety of fields ranging from the orbit of celestial object (the Moon and the Sun, for instance) to the mixing of the oceans, from solid-Earth geophysics to coastal flooding [5,6,7]. In addition, the rapid growth of tide modes facilitates the spatial and ground measurements greatly [8,9,10,11]. In the past decades the understanding of tidal dynamics and energy dissipation was markedly improved[12], tide prediction becomes more accurate than before. All these appear to show that the physics of tide had been understood well. However, a strict investigation reveals there still is a big step towards the final fact.

1.2 Problems of the established tidal theories

The established tidal theories may divide into two parts: the equilibrium tide and the dynamic tide. The equilibrium tide was directly developed from Newton's law of gravity and may be outlined with such a paradigm: the Earth orbits about the centre of mass of the Earth-Moon system, this makes all particles of the Earth travel around in circles which have the same radius. The force responsible for these circular or curved movements is treated as centripetal force. The centripetal force necessary to maintain each particle of the Earth this revolution is the same as for the particle at the centre of the Earth. For those particles nearer the Moon, the Moon's gravitational attraction on them is greater than the centripetal force. For those further away the Moon, the Moon's gravitational attraction are weaker than the centripetal force. The difference of the centripetal force and the Moon's gravitational attraction is the tide-generating force [1]. The tide-generating force is further decomposed into two components respectively perpendicular and parallel to the Earth's surface. The vertical component can be compensated by the Earth's gravity, but the horizontal component cannot be counteracted by the Earth's gravity and therefore causes these particles to move along the direction of the force. The net result of the tidal forces acting on a watery Earth is to move water towards the position nearest to the Moon and farthest from the Moon. This eventually generates two bulges of elevated water surface in the Earth-Moon line and a depression of the water surface in a ring around the Earth halfway between the bulges [2,13]. For a site of the Earth's surface it passes the two bulges as the Earth spins on its axis, this yields two cycles of high and low water per day. The equilibrium tide yields several points that are against observation.

First of all, the two bulges result in an equality of two low waters and an inequality of two high waters at a site. As shown in Figure 1 (a), in the midway of the two bulges it mechanically forms a ring (marked with white) of lowest water, a site P passes through this ring at P_1 and P_2 and through the two bulges at P and P' as the Earth spins, two low waters of same size and two high waters of different size are determined per day. From a viewpoint of the globe, other sites such as N and Q, which are at different latitudes, also pass through this ring respectively at $N_1(N_2)$ and $Q_1(Q_2)$ to form two low waters of same size. On the whole, the frame of the two bulges requests the high waters at all sites to be different in size whereas the low waters to be same within a fixed day. Contrary to this, the low waters of the observed tides are different in size.

Secondly, the two bulges request the size of two successive high waters at a site which is at higher latitude to be developed reversely during a lunar month, namely, the size of one high water is increased (decreased) whereas the size of another is decreased (increased) when the Moon transfers between north and south. This behavior may be easily seen from Figure 1 (a). Refer to Pugh's work [1], the tide-generating force was developed into a formula below to describe the elevation of the sea surface.

$$H_{\mathrm{m}}=a(M_{\mathrm{m}}/M_{\mathrm{e}})[C_0(t)(3\sin^2\varphi_{\mathrm{p}}/2-1/2)+C_1(t)\sin2\varphi_{\mathrm{p}}+C_2(t)\cos^2\varphi_{\mathrm{p}}]$$
$$C_0(t)=(a/R_{\mathrm{m}})^3(3\sin^2d/2-1/2)$$
$$C_1(t)=(a/R_{\mathrm{m}})^3(3\sin2d\cos C_{\mathrm{p}}/4)$$
$$C_2(t)=(a/R_{\mathrm{m}})^3(3\cos^2d\cos2C_{\mathrm{p}}/4)$$

where H_{m}, a, M_{m}, M_{e}, φ_{p}, R_{m}, d, and C_{p} are respectively the elevation of the sea surface, the Earth's radius, the Moon's mass, the Earth's mass, the latitude of a particle at the sea surface, the distance of the Earth and Moon, the declination of the Moon, and the hour angle of the particle relative to the Moon.

Replace M_{m} and R_{m} respectively with M_{s} (the Sun's mass) and R_{s} (the distance of the Earth and Sun), the elevation of the sea surface H_{s} due to the effect of the Sun may be got. $H_{\mathrm{m}}+H_{\mathrm{s}}$ therefore represent the total elevation of the sea surface due to the influences of the Moon and Sun. Figure1(b) exhibits several tides expected from the tide-generating forces. Related parameters for this expectation is listed in Table 1. It can be seen that, at latitude 30°N the size of one high water of the expected tide increases or decreases when the size of another high water decreases or increases during the month; towards higher latitudes (60°N and 80°N, for instance) this asymmetry is developed considerably. Contrary to these, the tide records in Figure 1(c) show that the two successive high waters of each of the observed tide are

alternately increased or decreased, this behavior is also applicable for the two successive low waters. On the whole, there is a big discrepancy of morphology between the expected tides and the observed tides.

Thirdly, according to Figure 1(a), the two bulges request semidiurnal tides (two high waters and two low waters per day, and the size of two high or low waters is equal) to occur at lower latitudes (equator, for instance), diurnal tides (one high water and one low water per day) to occur at higher latitudes, and mixed tides (two high waters and two low waters per day, but the size of two high or low waters is not equal) to occur at middle latitudes. Contrary to this, the tide records in Figure 1(e) reveal that the distributions of semidiurnal and mixed tides are almost dominant around the globe, there are only a few places (the Karumba gulf, the Mexico gulf, for instance) owning diurnal tides.

Lastly, there is a significant tidal range difference between the ocean tides and the continental shelf tides. The tidal range calculated from the tide-generating forces is 0.5 m at equator. However, the observed tides in the main oceans have average ranges of about 0.0~1.0 m, while in the continental shelf seas much larger tidal ranges are observed. At some places (the Bay of Fundy and the Argentine shelf, for instance) the tidal ranges may be greater than 10.0 m [1].
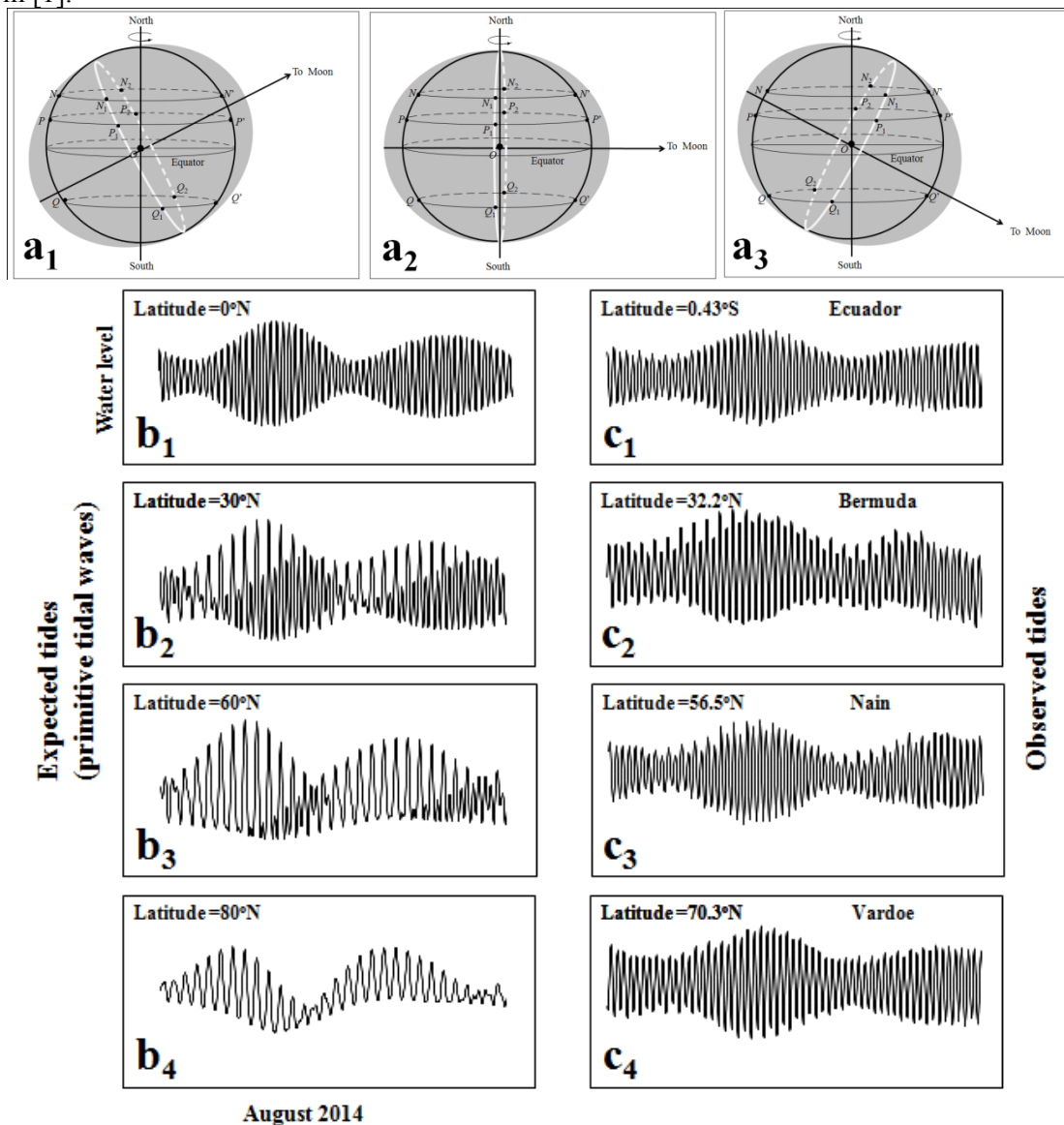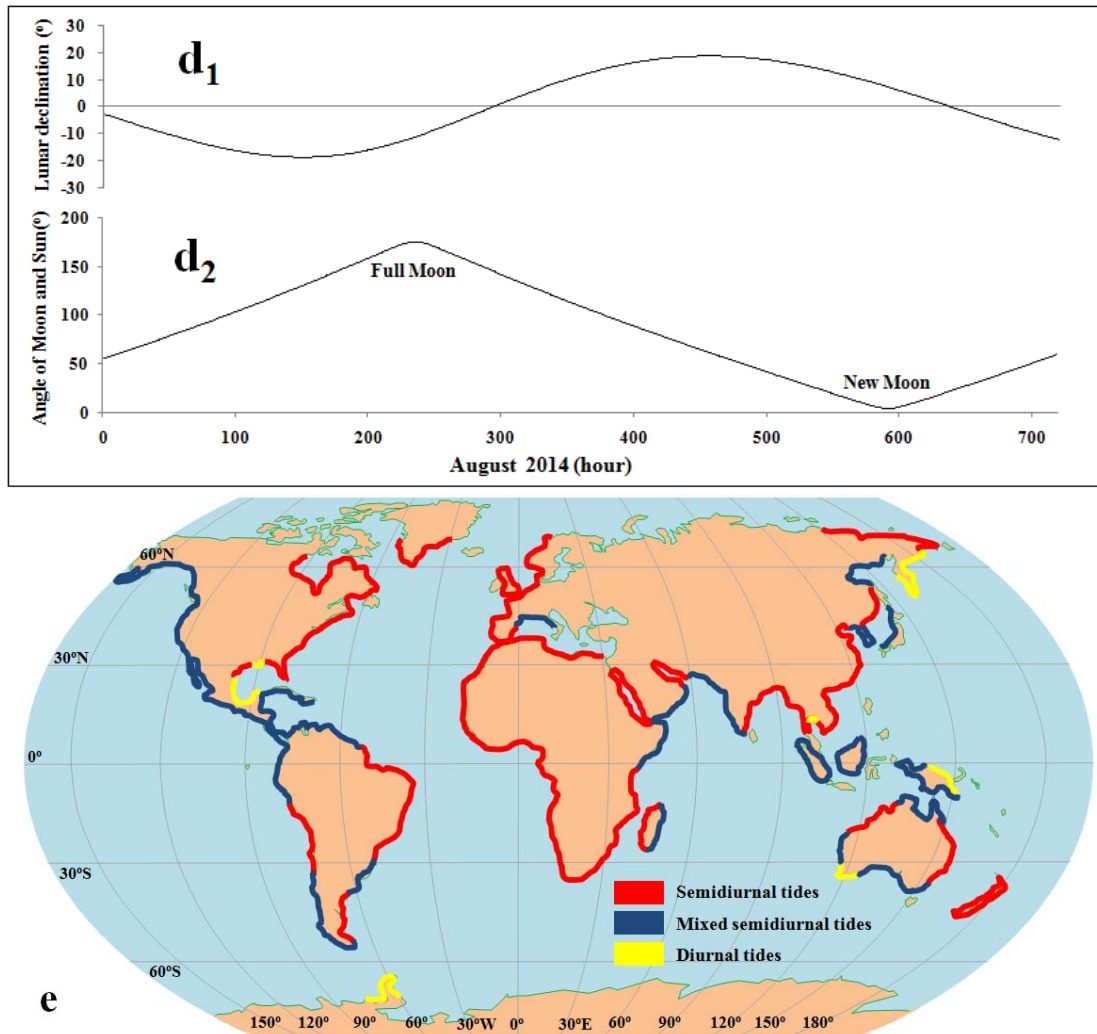
Figure 1: Comparison of the expected tides from the attractive mechanism and the observed tides. a, showing how the unequal high waters and the equal low waters are generated at various sites under the resulting two bulges. From a_1, a_2, to a_3, it orderly represents the positions of the two bulges as the Moon transfers from the north to the south. *O* is the Earth's centre. Big circle represents undisturbed watery planet. Note the structure of the two bugles is seriously exaggerated; **b**, the expected tides at different latitudes in August 2014. They are got through the tide-generating force and also represent the primitive tidal waves; **c**, the observed tides at different latitudes during the month; **d**, the positions of the Moon and Sun relative to the Earth in the month; **e**, tidal pattern distribution of the observed tides throughout the globe. Data supporting this map are from U.S. NOAA, GLOSS database (University of Hawaii Sea Level Center), and Bureau National Operations Centre (BNOC) of Australian government.

Several factors had not been considered in the equilibrium tide. If no landmass, the tidal bulges would continuously track from east to west as the Earth spins day by day. But the presence of landmasses breaks off this progression. Most of continents are oriented north-south, the travelling tidal wave would encounter continent, generating a reflection of tidal wave. From deep oceans to shelf seas the water depth becomes shallow, the slop of seafloor may disperse and refract tide wave greatly. One consequence of the Coriolis force is to deflect tidal wave to the right of the direction of motion in the northern hemisphere and to the left of the direction of motion in the southern hemisphere. With the constraint of these influences, the dynamic tide was developed by scientific community. An earlier treatment on

this matter was made by Laplace who in 1775 expanded the equilibrium tide into a set of hydrodynamic equations of continuity and momentum. Laplace assumed a spherical Earth with a geocentric gravitational field, a rigid ocean bottom and a shallow ocean which allowed Coriolis accelerations to be neglected [1]. These hydrodynamic equations created foundation for the following developments of a series of ideas such as progressive and standing wave, resonance, Kelvin wave, and amphidromic system. Wave has the characteristics of crest (high) and trough (low), this resembles the shape of high and low water, hence, treating tide as wave is theoretically acceptable. Wave may propagate or be reflected, and two waves may interfere, especially resonating to amplify if their frequency is close to each other. Based on these properties, a general understanding is achieved: ocean tides were generated directly by the external gravitational forces, the continental shelf tides were generated by co-oscillation with oceanic tides [1]. However, some critical problems keep unresolved in the dynamic tide.

Firstly, the dynamic tide itself is based on an assumption that ocean bottom is rigid, this means ocean bottom can't be deformed by the external gravitational force. In reality the elasticity of solid Earth means ocean bottom is deformable. The rise and fall of each part of ocean bottom can mechanically give rise to a decrease and increase of water depth as solid Earth spins. This therefore leads to a problem, it is difficult to differentiate whether the external gravitational force directly drives ocean waters to form tides or the external gravitational force indirectly drives ocean bottom to form tides or both.

Secondly, the sources of the semidiurnal tides at middle and high altitudes remain unclear. Before we discuss the movement of tidal wave, we need to know two points well: how does tidal wave form and what's its primitive form? Because the tide-generating forces eventually yield two bulges for the Earth, an earthly site has to pass through these bulges as the Earth spins, and hence, undergoes a movement of rise (high) and fall (low). Once this movement is treated as progressive wave, this means tidal wave is launched from east to west and its primitive form is just the shape of the tide generated by the tide-driving forces. As shown in Figure 1(b), at middle and high altitudes the shapes of the tides generated by the tide-driving forces are non-sinusoidal, and at equator they are somewhat sinusoidal. A sinusoidal wave has the property that the height of its crest is equal to that of its trough. Strictly speaking, the shapes of the tides generated by the tide-driving forces would be sinusoidal at the time when both the Moon and the Sun are at equator. However, this chance is extremely rare, in most cases the two bodies lie at either the north or the south. After tidal waves are launched to travel they would be dispersed, refracted, and reflected by the continents they meet, the Coriolis effect also may deflect them, but physically, these actions wouldn't change their primitive shapes. Therefore, an oncoming problem is where the observed semidiurnal tides (which are sinusoidal) at middle and high altitudes come from or how they form. A way is to transfer the equatorially semidiurnal tidal waves towards these places, but practically it is difficult. The equatorially semidiurnal tidal waves can't be deflected by the Coriolis effect unless their propagating directions are firstly changed. For the Pacific ocean, the westward equatorially semidiurnal tidal waves would arrive at Indonesian seas, from where they can be dispersed by a pile of cluttered islands, a leading deflection towards the north or towards the south becomes impossible. For the Atlantic ocean, the westward equatorially semidiurnal tidal waves would be refracted by the landmass along Brazil towards the north, and subsequently, are deflected by the Coriolis effect. A result from these two successive actions is there will be a progression of tidal phases along the path. But observations disapprove this expectation. The phases are nearly constant along the whole coast of northern Brazil from 35°W to 60°W. Along the Atlantic coast of North America from Nova Scotia to Florida the tides are nearly in phase [1]. The northern Brazil is oriented northwest-to-southeast, this means the westward equatorially semidiurnal tidal waves can't be refracted towards the south, hence, the semidiurnal tides at South Atlantic lost their sources. From another point of view, the energy represented by the equatorially semidiurnal tidal waves is too less to balance the energy represented by the observed semidiurnal tides around the globe. Another way is to synthesize them at local, but practically it is also difficult. This is because the combination of two sinusoidal waves may yield a sinusoidal or non-sinusoidal wave, whereas the combination of one sinusoidal wave and one non-sinusoidal wave or the combination of two

non-sinusoidal waves can't yield a sinusoidal wave. Once the sources of the semidiurnal tides at middle and high altitudes can't be found, the current tide prediction will become groundless.

Lastly, suppose the oceanic tidal waves have smoothly spread onto the continental shelf seas, however, their resonances with local oscillations are still not easy to happen. This is because, the resonance of two waves has a strictly physical constraint, an approach of frequency (also wavelength) is simply not enough. At least, the phase of two waves must be the same. For example, if the wavelengths of two sinusoidal waves are the same but the phase between them has a difference of 180°, the amplitude of the combined wave would be zero. This point may be demonstrated with the composition of two sinusoidal waves $\sin(2\omega t)$ (the natural) and $\sin(2\omega t + k45)$ (the forced), which resemble semidiurnal tide, the natural and the forced conceptually represent the oscillation of the continental shelf sea and the oceanic tidal wave, respectively, where ω is angular speed of unit degree per hour, and $\omega = 15^o$, t is time of unit hour, $k45$ is phase lag of unit degree, $k=0, 1, 2, 3, 4, 5, 6, 7$, and 8. It can be seen in Figure 2 that the amplitudes of some of the combined waves are greatly suppressed when phase lag is between $135^o \sim 225^o$, in particular, the amplitude reduces to zero when phase lag is 180°. These amplitudes can be amplified when phase lag is between $0^o \sim 135^o$ and between $225^o \sim 360^o$.
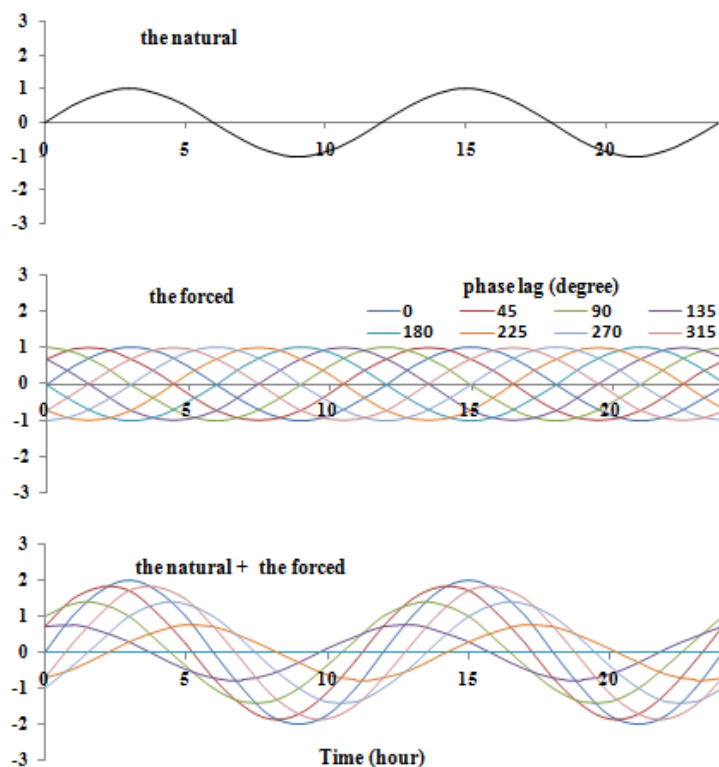
Figure 2: Modelling a resonance between natural oscillation and forced oscillation under different phase lag.

The demonstration above leads to the fact that a system, which is forced by oscillation close to its natural period, is unnecessary to yield large amplitude anywhere. One must be aware that, due to the Moon's advance in its orbit, the gravitational pull of the Moon on an Earthly site has a phase (time) lag of about 52 minutes per day (equivalent to 3.75^o per day). This means that, after 36 days the total phase lag falls into a span of $135^o \sim 225^o$, in which a counteraction of the forced and the natural will be done. In other words, to realize the resonance of the oceanic tidal wave and the natural oscillation of the continental shelf sea, the latter has to timely recede so as to keep synchronization with the former. This hence leads to a problem why the natural oscillation of the continental shelf sea may recede day by day. It is unintelligible because we never heard that the natural (inherent) oscillation of a system will

advance or recede. One must also be aware that, in real world the occurrences of resonated events (collapsing bridge, acoustic speaker, for instance) are markedly rare, there has no eternal resonance for a special system. Attempting to relate resonance to tide appears to violate our intuition.

2 A reconsideration of the tide
2.1 An analytic treatment of the deformation of solid Earth
The Earth may be mechanically thought to be a solid sphere that is enveloped by water and atmosphere[14,15,16]. The structure of solid Earth, from surface to interior, is sequentially divided into crust, mantle, outer core, and inner core[17]. A large number of works confirmed that these layers are filled with various materials [18-23] and denser materials are gravitationally concentrated towards the interior[24]. Notwithstanding, solid Earth is strictly not a rigid body, both experiments and measurements had proved it to be elastic[25, 26] and to had been stretched into an oblate spheroid because of a centrifugal effect of the Earth's rotation about its axis [27,28]. This suggests, solid Earth can be deformed by a centrifugal effect. It is well known that the Earth orbits about the centre of mass of the Earth-Moon system and the Earth-Moon system orbits about the Sun. A fuller details of the movements of the Earth, Moon, and Sun may be seen in these works [29-34]. These two curved movements generate two centrifugal effects F_1 and F_2 for solid Earth (Figure 3(a_1)). F_1 and F_2 are respectively balanced by the gravitational attraction from the Moon f_1 and from the Sun f_2. If we define the centrifugal effect of the Earth's rotation about its axis as F_3, then the ratio between F_1, F_2, and F_3 will be 1:178:505 according to established parameters such as orbital radius, orbital period, mass of each body, and so on. Practically, F_2 is far greater than F_1, but the working point of F_2 is not at the Earth's centre, compared to the working point of F_1 that is at the Earth's centre. In consideration of this matter, we suppose the effective part of F_2, which is able to stretch the Earth, is relatively small and lies at the Earth centre (O_1). The counteraction of F_1 (F_2) and f_1 (f_2) finally leads solid Earth to be elongated in the Earth-Moon (Sun) line (Figure 3(a_2 and a_3)). We call it lunar (solar) deformation in the following sections. Under the frame of such deformation, an Earthly site will undergo a change of rise and fall as the Earth spins on its axis.

To better run the following deduction, we assume solid Earth to be a standard sphere and use the centrifugal effects F_1 and F_2 to independently stretch solid Earth along the Earth-Moon line (O_1M) and the Earth-Sun line (O_1S). Suppose a case, if an elastic ball is mechanically stretched along a fixed direction, forming two bulges, and then, the ball will be accordingly shortened in the midway between the bulges. For solid Earth (which is elastic) it can also bear such a behavior. Under the centrifugal effect F_1, section GIHJ which passes through an Earthly site M becomes section G'I'H'J', section KQLP becomes section K'Q'L'P', site M turns to site M'. Section GIHJ is geometrically perpendicular to section KQLP, GH is the intersecting line between them (Figure 3(b_1, b_2, and b_3)); Under the centrifugal effect F_2, section VSWR which also passes through site M and section TYUX respectively become sections V'S'W'R' and T'Y'U'X', site M turns to site M'', section VSWR is perpendicular to section TYUX, VW is the intersecting line between them (Figure 3(c_1, c_2, and c_3)). It can be seen that solid Earth simultaneously undergoes two elongations (in the direction of the Earth-Moon line and in the direction of the Earth-Sun line) and two compressions (in the direction of section KQLP and in the direction of section TYUX). Hence, the final position of site M relative to the Earth's centre is a result of the combination of these adjustments (elongations and compressions). According to the geometry of ellipse, the distance of site M and the Earth's centre may be expressed as

$$H = O_1M' + O_1M'' - O_1M \quad (1)$$
$$O_1M' = [I'O_1{}^2\cos^2\beta + G'O_1{}^2\sin^2\beta]^{1/2} \quad (2)$$
$$O_1M'' = [S'O_1{}^2\cos^2\gamma + V'O_1{}^2\sin^2\gamma]^{1/2} \quad (3)$$

Where

$I'O_1$ and $G'O_1$ are the semi-major and semi-minor axis of ellipse G'I'H'J', respectively, and $GO_1 = IO_1$, $G'O_1 = GO_1 - k_m'$, $I'O_1 = IO_1 + k_m$, k_m is the elongation of solid Earth in the

direction of the Earth-Moon line (O_1M) that is due to the centrifugal effect F_1, k_m' is the compression of solid Earth in the direction of section KQLP, GO_1 (IO_1) is the mean radius of solid Earth, equal to O_1M. β is the angle of site M and the Moon relative to the Earth's centre.

S'O_1 and V'O_1 are the semi-major and semi-minor axis of ellipse V'S'W'R', respectively, and VO_1= SO_1, V'O_1= VO_1-k_s', S'O_1= SO_1+k_s, k_s is the elongation of solid Earth in the direction of the Earth-Sun line (O_1M) that is due to the centrifugal effect F_2, k_s' is the compression of solid Earth in the direction of section TYUX, VO_1 (SO_1) is the mean radius of solid Earth, equal to O_1M. γ is the angle of site M and the Sun relative to the Earth's centre.

β and γ are calculated through some astronomical constants. cos β = sinσsinδ_m + cosσcos$\delta_m$cosC_{mm}, cosγ= sinσsinδ_s + cosσcos$\delta_s$cosC_{ms}, where σ, δ_m, δ_s, C_{mm}, and C_{ms} are respectively the geographic latitude of site M, the declination of the Moon, the declination of the Sun, the hour angle of site M with respect to the Moon, and the hour angle of site M with respect to the Sun. The declination and right ascension of the Moon and the Sun may be got from ephemeris or be calculated, the hour angle may be worked out through the positions of these bodies.
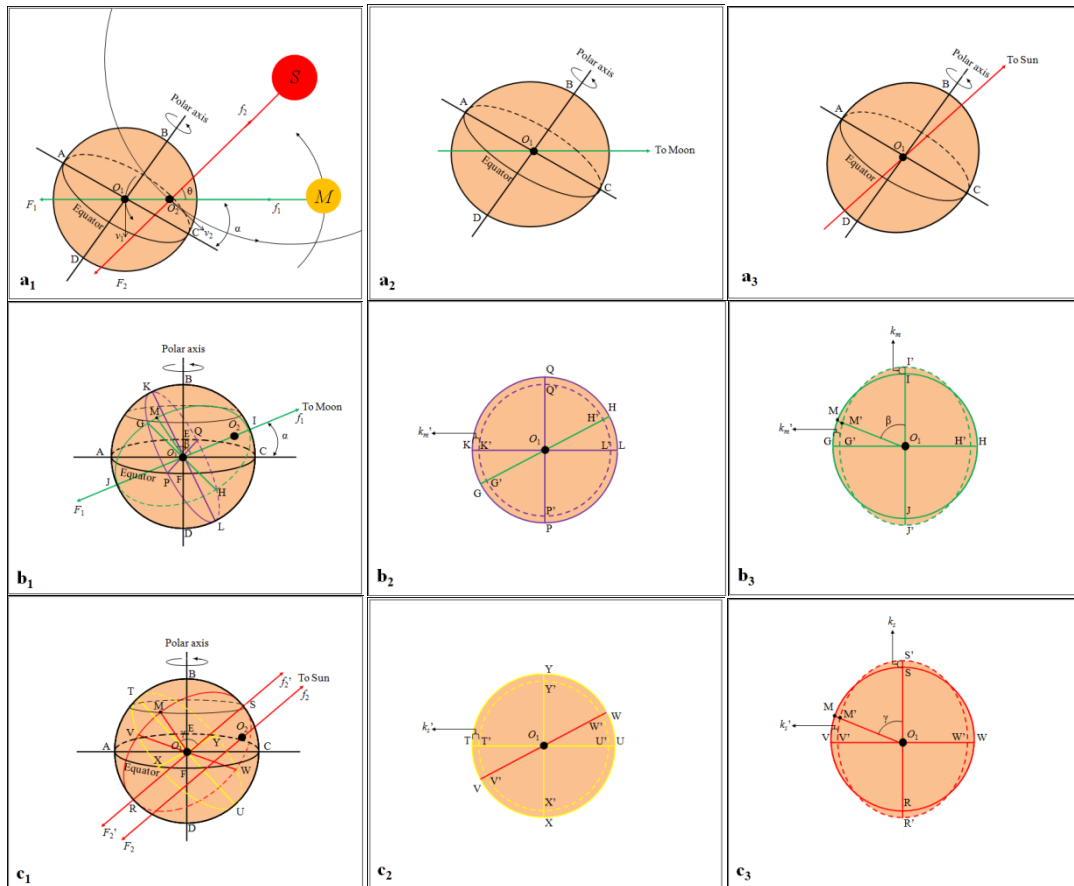
Figure 3. Combined centrifugal effects for solid Earth and the resulting deformation. a₁, the curved motions of the Earth around the barycenter of the Earth-Moon system and around the Sun, **a₂** and **a₃** are the resulting deformations respectively in the direction of the Earth-Moon line and in the direction of the Earth-Sun. F_1 and F_2 are the centrifugal effects solid Earth undergoes due to these curved motions. O_1, O_2, M, and S are the Earth's centre, the barycenter of the Earth-Moon system, the Moon, and the Sun, respectively. Θ is the angle between the Moon and the Sun relative to the barycenter of the Earth-Moon system. Section AECF is the equatorial plane, α is the Moon's declination. v_1 and v_2 are respectively the velocity of the Earth orbiting the barycenter of the Earth-Moon system and the velocity of the Earth-Moon system orbiting the Sun, which generate the centrifugal effects F_1 and F_2 that are anywhere balanced the gravitational attraction from the Moon f_1 and from the Sun f_2; **b₁, b₂,** and **b₃,** solid Earth under the effect of F_1 and the resulting deformations respectively in the direction of section KQLP and in the direction of the Earth-Moon line. Purple (green) real and dashed circles represent the original and disturbed shapes of solid Earth in the related directions; **c₁, c₂,** and **c₃,** solid Earth under the effect of F_2 (also F_2') and the resulting deformations respectively in the direction of section TYUX and in the direction of the Earth-Sun line. Line F_2'f_2' is

parallel to line F_2f_2, meaning the centrifugal effect F_2 and gravitational attraction f_2 are working on the Earth's centre (O_1). Yellow (red) real and dashed circles represent the original and disturbed shapes of solid Earth in the related directions.

The ratio of centrifugal effect F_3/F_1 is about 505:1. A rough evaluation based on this amount is the centrifugal effect F_1 may generate an elongation of about 42.00 m for solid Earth if the Earth's oblate spheroid is referred. However, the Earth's oblate spheroid is likely to be resulted from an accumulative effect during a time scale of billions of years, thus, the centrifugal effect F_1 at instant could give rise to only a slight amount. Here we assume the elongation of solid Earth in the Earth-Moon line (due to the centrifugal effect F_1) at instant to be 0.50 m at the time when the Moon is at perigee and in the Earth-Sun line (due to the centrifugal effect F_2) at instance to be 0.30 m, and assume the response of the compression to the elongation to be a factor of 1.0. The Moon's elliptical orbit means a timely changing distance between the Earth and the Moon. As the centrifugal effect F_1 is anywhere balanced by the Moon's gravitation and the Moon's gravitation is reversely proportional to the square of distance, the elongation of solid Earth in the Earth-Moon line may thus be approximately expressed as $k_m=0.5R_m^2/R_{peri}^2$. For the elongation of solid Earth in the Earth-Sun line it may be constant because the Earth's orbit is nearly circular. And then, $k_s=0.30$ m, $k_m'=k_m$, $k_s'=k_s$, where k_m and k_s are respectively the elongation of solid Earth in the Earth-Moon line and in the Earth-Sun line, k_m' and k_m' are respectively the compressions to the response of the elongations. Please note, practically the elongation k_m (k_s) and compression k_m'(k_s') should be obtained by means of measurement.

The final deformation of solid Earth is therefore a result of the combination of lunar and solar deformation, and may periodically vary due to the changes of the positions of the Moon, Sun, and Earth. In particular, it becomes maximal at the times of full and new Moon and minimal at the times of first quarter and last quarter. This is because at the times of full and new Moon the two deformations add each other to reinforce, whereas at the times of first quarter and last quarter the two cancel each other to weaken.

2.2 The water movement of an oscillating vessel
As shown in Figure 4, we firstly let the right end of a rectangular water box rise, the water then flows towards left. If line MN represents a reference level, during this course the water level at site M rises whereas the water level at site N falls. We further restore right end to its former level and continue to let the left end rise, the water at left end flows towards right, the water level at site M correspondingly falls whereas the water level at site N rises. Repeat the rise and fall of the two ends continuously, the water level of sites M and N alternately vary. Compared to sites M and N, another site S, which is in the middle of the vessel, holds the minimal variation of water level. Now we let one end rise and fall continuously but another end ideally keeps motionless, the water level at sites M and N still alternately vary. Further, we let one end rise (fall) and another end fall (rise) at the same time, the water level at sites M and N also alternately vary. The variation of water level at one end may be approximately represented by the difference of vertical displacement between the two ends. Mathematically, this behavior of the movements of high and low water at an oscillating vessel may be depicted with a sinusoidal wave.
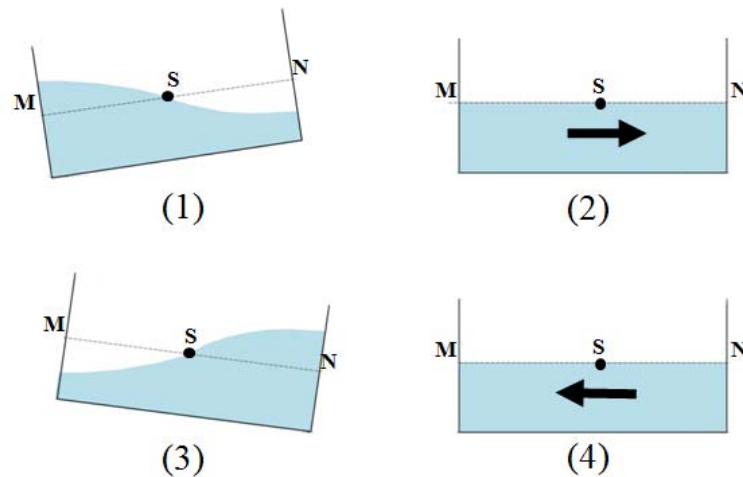
Figure 4. Modelling the water movement of an oscillating rectangular box. From (1), (2), (3) to (4) it represents a full alternation of the rise and fall of the two ends. Arrows denote the directions of water movements.

2.3 The resulting tide

Turn to real world, about 71% of the Earth's surface is covered with ocean water [35]. In appearance, all the oceans bisect the Earth's surface, and each ocean basin is like a gigantic vessel of water. According to the arguments we presented above, due to the deformation of solid Earth, every part of ocean basin would rise and fall regularly as the Earth spins, this mechanically generates water transferring back and forth, and also high and low water at the ends of ocean basin per day. This movement of water transferring may be depicted with Figure 6. Within the lunar deformation of solid Earth, there is an elongation in the direction of the Earth-Moon line and a compression in the midway of the elongation. The elongation may be represented by two bulges. The first bulge would track from east to west along line L as the Earth spins. For a coastal site W, the raising of site a firstly leads water to move towards site W, subsequently, the raisings of the site b, c, and d, which are assumed to be located at the bottom of the ocean, lead water to move out from these sites, at least, there is a water transferring from each of these sites to site W. With the passage of time, site a, b, c, and d begin to fall by order, this leads water to move in, at least, there is a water transferring from site W to each of these sites. Half a day (about 12 hours) later, the second bulge would track from east to west along line L', the raisings of site e, f, g, and h (site f and g are also assumed to be located at the bottom of the ocean), lead water to move out from these sites, at least, there is a water transferring from each of these sites to site W. Similarly, with the passage of time, these sites begin to fall by order, this leads water to move in, at least, there is a water transferring from site W to each of these sites. Please note, in the day each of site b, c, d, f, and g would undergo a maximal rising and would also undergo a maximal falling. Even if site a, e, and h can't undergo a maximal rising, but the landmass's raising still would lead water to move from these sites to site W, this may ascribe to a spherical structure of the Earth. Once the water transferring between site W and each of these sites is treated as wave, the total variation of water level at site W may be expressed with a simple addition of all these waves. This therefore provides foundation for the following and established tide prediction.
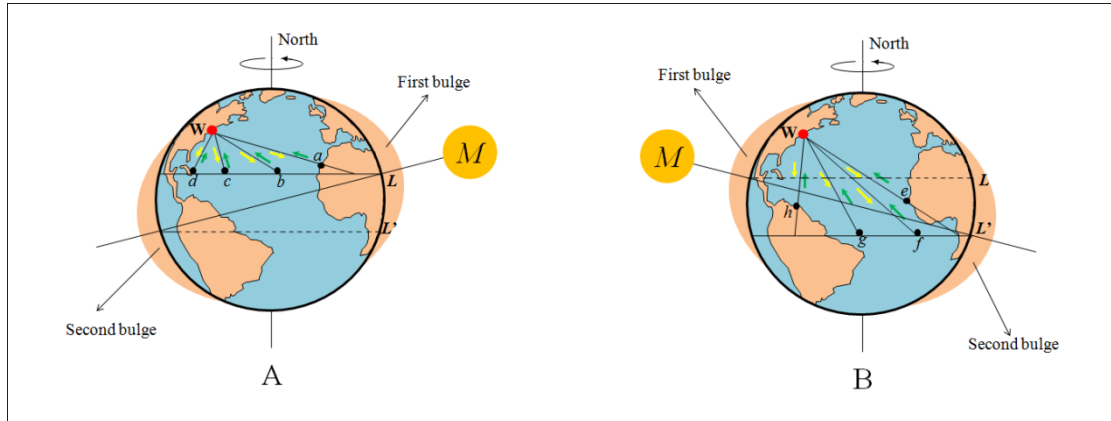
Figure 6. A simplified system illustrates water transferring due to the rises and falls of related sites. From A to B, it means the Earth rotates 180° with respect to the Moon. Green and yellow arrows denote the directions of water transferring between site W and these sites. *L* (at the far side) and *L'* (at the near side) represent the paths the Earth-Moon line tracks along the Earth's surface. The two bulges denote the elongation of solid Earth

Four sites (Karumba, Fort Point, Prince Rupert, Rorvik) are selected to perform the variation of water level. In consideration of the physics of the oscillating rectangular vessel and of the water transferring in the ocean, each of these sites acts as one end of a smaller rectangular vessel, one and more partners are employed for acting as another ends of these smaller vessels. The treatments of these vessels are outlined in Figure 7(a). V_{11}, V_{21}, V_{31}, and V_{41} represent the four sites, V_{12}, $V_{22}(V_{22}')$, V_{32}, V_{33}, V_{34}, V_{35}, V_{36}, and V_{42} are their first partners. V_{13} is added as second partner of V_{11} because the rising or falling of V_{13} (which is at the northwest Celebes Sea) would lead water to transfer between V_{13} and V_{12}, from V_{12} the transferring water can further move towards V_{11} or V_{13}. V_{32}, V_{33}, V_{34}, V_{35}, and V_{36} are added as first partners of V_{31} because the risings or fallings of these sites all would lead water to transfer between V_{31} and them. V_{43}, V_{44}, V_{45}, and V_{46} are added as second partners of V_{41} because the risings or fallings of these sites all would lead water to transfer between V_{42} and them, from V_{42} the transferring water can further move towards V_{41} or these sites. As we demonstrated above, the maximal rising of solid Earth is always in the direction of the Earth-Moon line and the paths the Earth-Moon line tracks the Earth are along *L* and *L'*, this means that the positions of V_{22}, V_{32}, V_{33}, V_{34}, V_{35}, V_{36}, V_{43}, V_{44}, V_{45}, and V_{46} are timely variable, relevant to the position of the Moon. Some possible positions for them are marked with V_{22}', V_{32}', V_{33}', V_{34}', V_{35}', V_{36}', V_{43}', V_{44}', V_{45}', and V_{46}'. Through Google earth software we figure out the geographic latitudes and longitudes of V_{11}, V_{12}, V_{13}, V_{21}, V_{31}, V_{41}, and V_{42}. The determination of the geographic latitudes and longitudes of $V_{22}(V_{22}')$, $V_{32}(V_{32}')$, $V_{33}(V_{33}')$, $V_{34}(V_{34}')$, $V_{35}(V_{35}')$, $V_{36}(V_{36}')$, $V_{43}(V_{43}')$, $V_{44}(V_{44}')$, $V_{45}(V_{45}')$, and $V_{46}(V_{46}')$ is relatively complicated. Taking into account the paths that the Earth-Moon line tracks on the Earth's surface, the latitude of $V_{22}(V_{22}')$ is treated the same as the positive of the Moon's declination if the angle between V_{21} and the Moon relative to the Earth's centre is less than 90° and the same as the negative of the Moon's declination if the angle is greater than 90°, the longitude of $V_{22}(V_{22}')$ is treated the same as that of V_{21}; the latitudes of $V_{32}(V_{32}')$, $V_{33}(V_{33}')$, $V_{34}(V_{34}')$, $V_{35}(V_{35}')$, and $V_{36}(V_{36}')$ are treated the same as the positive of the Moon's declination if the angle between V_{31} and the Moon is less than 90° and the same as the negative of the Moon's declination if the angle is greater than 90°, their longitudes are designed to have a difference of 15°, 0°, -15°, -30°, and -45° towards the longitude of V_{31}; the latitudes of $V_{43}(V_{43}')$, $V_{44}(V_{44}')$, $V_{45}(V_{45}')$, and $V_{46}(V_{46}')$ are treated the same as the positive of the Moon's declination if the angle between V_{42} and the Moon is less than 90° and the same as the negative of the Moon's declination if the angle is greater than 90°, their longitudes are designed to have a difference of 10°, 5°, 0°, and -5° towards the longitude of V_{42}. Once the geographic latitudes and longitudes of these sites are got, the distance between any of these sites and the Earth's centre may be calculated through the formula (1), (2), and (3). And then, O_1V_{13} - O_1V_{12} + O_1V_{12} - O_1V_{11}, $O_1V_{22}(O_1V_{22}')$ - O_1V_{21}, $O_1V_{32}(O_1V_{32}')$ + $O_1V_{33}(O_1V_{33}')$ + $O_1V_{34}(O_1V_{34}')$ +

O_1V_{35} (O_1V_{35}') + O_1V_{35} (O_1V_{35}') - O_1V_{31}, and O_1V_{43} (O_1V_{43}') + O_1V_{44} (O_1V_{44}') + O_1V_{45} (O_1V_{45}') + O_1V_{46} (O_1V_{46}') - O_1V_{42} + O_1V_{42} - O_1V_{41} approximately represent the variation of water level at site V_{11}, V_{21}, V_{31}, and V_{41}. We see, V_{12} and V_{42} just play a role of connecting point. In the experiment of the oscillating vessel we found that, with the passage of time, the rise or fall of water level at one end can't timely response to the rise or fall of another end, there is often a lag of time between them, time lag is therefore considered for some of these vessels. In practice there is usually a delay of a day or two between full and new Moons and the following spring tides, this is called the age of tide, and also is considered for all these vessels. The reason for this delay could be due to the inertia of transferring water that is globally acted.

The deformation of solid Earth we propose requests gravity to vary from site to site. Three sites (Strasbourg, Sutherland, and Apache Point) are selected to examine this expectation. Gravity variation (g) is calculated by a formula $g \sim 1/r^2 - 1/a^2$, r is the distance between any of three sites and the Earth's centre, which can be got through the formula (1), (2), and (3) if the geographic latitudes and longitudes of these sites are known, a is the mean radius of the Earth. The simulated and observed tides (gravity variation) are shown in Figure 7(b and c). Related parameters used in the simulation are listed in Table 1. On the whole, the simulated results are morphologically well consistent with the observed results. But for a more exactly tidal prediction, some factors such as the shape of ocean basin, orientation of coastline, water depth, Coriolis effect, inertia, and so on should be included, in particular, once ocean basin is divided into a series of smaller vessels, the input of water from adjacent vessels needs to be included, this is because the travelling water at one vessel may be refracted or reflected to enter another vessel.
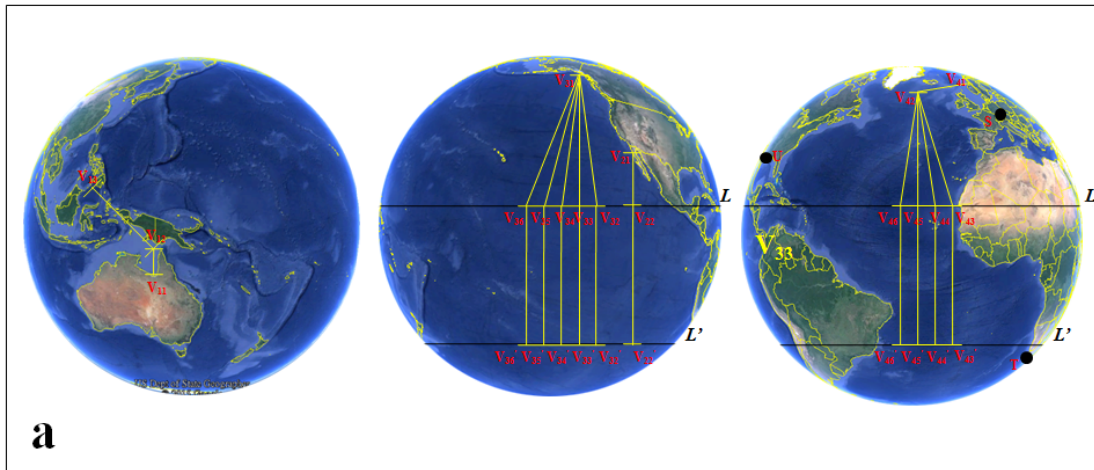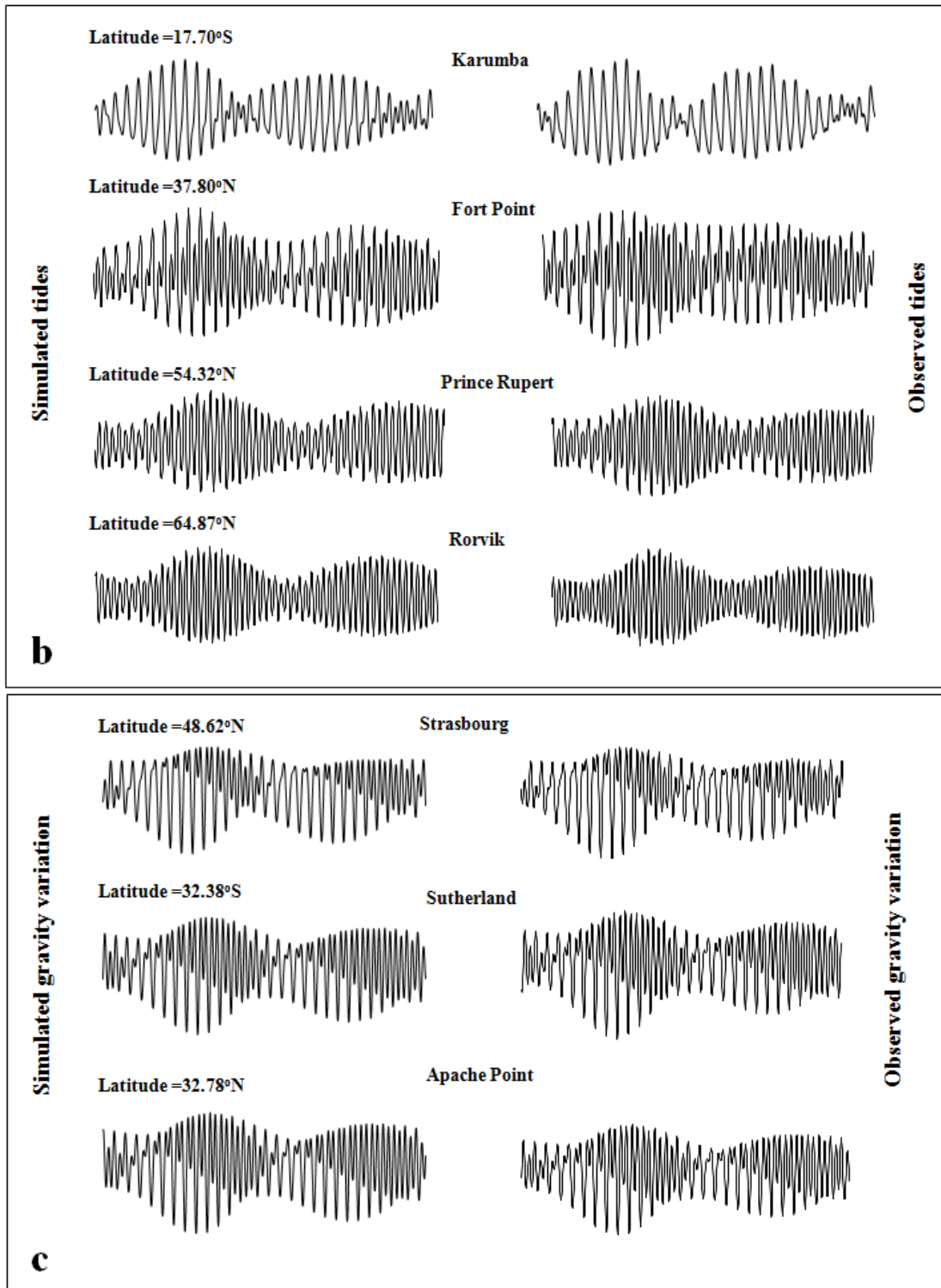
Figure 7. Treatments of ocean vessels and comparisons of simulated and observed results. a, defining smaller vessels within ocean basins and putting GGP (Global Geodynamics Project) sites at the surface of solid Earth (base map is from Google Earth). V_{11}, V_{12}, …, represent the ends of the wanted vessels. Each rectangular box represents a smaller vessel. S, T, and U represent three gravity observational sites. *L* and *L'* are the expected paths that the Earth-Moon line tracks the Earth, which give the latitudinal scope of the maximal rising point; **b**, showing a morphological comparison of the simulated and observed tides without scale in August 2014. In the simulation time lag for Fort Point is 2.0 hours, and for Prince Pupert, which involves in fives partners, is averagely 2.0 hours. The age of tide is commonly accepted as 2 days (about 48 hours); **c**, showing a morphological comparison of the simulated and observed gravity variations. Time span for all these simulations is from UTC 2014-08-01 00:00:00 to 2014-08-30 23:00:00. The lunar and solar ephemeris are from JPL HORIZONS system.

13

Water level data is from GLOSS database (University of Hawaii Sea Level Center) and Bureau National Operations Centre (BNOC) of Australia. Gravity data (made by supergravimeter) is from GGP (Global Geodynamics Project).

Table 1   **Parameters selected for simulation**

The Moon			Symbol
	Mass	$7.35*10^{22}$ kg [36]	M_m
	Perigee	362600 km	R_{mp}
	Apogee	405400 km	R_{ma}
The Earth			
	Mass	$5.97*10^{24}$ kg [37]	M_e
	Mean radius	6370 km [38]	a
	Mean distance from Sun	149597870 km [39]	R_s
The Sun			
	Mass	$1.99*10^{30}$ kg [40]	M_s
Geographic sites for water vessels		Latitude, Longitude	
	Karumba, Austrilia	17.70°S, 139.20°E	V_{11}
	Partner (1)	13.00°S, 141.00°E	V_{12}
	Partner (2)	5.00°N, 121.00°E	V_{13}
	Fort Point, San Francisco, USA	37.80°N, 122.47°W	V_{21}
	Partner (1)	__, 122.47°W	$V_{22}(V_{22}')$
	Prince Pupert, Canada	54.32°N, 130.32°W	V_{31}
	Partner (1)	__, 115.32°W	$V_{32}(V_{32}')$
	Partner (2)	__, 130.32°W	$V_{33}(V_{33}')$
	Partner (3)	__, 145.32°W	$V_{34}(V_{34}')$
	Partner (4)	__, 160.32°W	$V_{35}(V_{35}')$
	Partner (5)	__, 175.32°W	$V_{36}(V_{36}')$
	Rorvik, Norway	64.87°N, 11.25°E	V_{41}
	Partner (1)	50.00°N, 28.00°W	$V_{42}(V_{42}')$
	Partner (2)	__, 18.00°W	$V_{43}(V_{43}')$
	Partner (3)	__, 23.00°W	$V_{44}(V_{44}')$
	Partner (4)	__, 28.00°W	$V_{45}(V_{45}')$
	Partner (5)	__, 33.00°W	$V_{46}(V_{46}')$
Geographic sites for gravity		Latitude, Longitude	
	Strasbourg, France	48.62°N, 7.68°E	S
	Sutherland, South Africa	32.38°S, 20.82°E	T
	Apache Point, New Mexico, USA	32.78°N, 105.82°W	U

3 Discussion

The mechanism of the oscillating water vessel is also applicable for the matter of the enclosed sea/lake. If we treat Black sea as a vessel and use formula (1), (2), and (3) to estimate, the west or east end of this sea may experience a tide of about 12.0 cm. Similarly, a tube of water (20 m in length) horizontally located at equator will experience a tide of about 2.2×10^{-3} mm, an imperceptible amount. This means that, any small vessel, such as swimming pool, water cup, water bowl, and so on, because of its short size, wouldn't undergo an perceptible tide. The oscillation of ocean basin drives water to move, continental shorelines are long enough to block the coming water to form large accumulation. In particular, most of the shorelines are concave, this also may create an effect of narrow to amplify tide. Typical representatives are the tides around Qiantang River and Bay of Fundy. In contract, the shorelines of the islands that are fully isolated in the deep oceans are short, the coming water can't be accumulated and may bypass. These determine larger tidal ranges to occur at the coastal seas and smaller ones to occur at the deep oceans. The rotating deformed solid Earth drives ocean water to move back and forth. The transferring water in travel, if constrained by the narrowness of strait, may form swift current, like that in the Cook Strait [41,42]. For the various features of the tides in the Atlantic and in the North West Europe shelf seas, they may be understood as follows: the rising and falling of each part of ocean basin are in a manner of from east to west as the Earth spins, the rising of east end of the Atlantic basin firstly leads water to flow towards north, west, and south, the following rising of middle part of the Atlantic basin leads water to flow towards east, north, west, and south, finally, the rising of west end of the Atlantic basin leads water to flow towards north, east, and south. The westerly water may reach the eastern coastline of America nearly at the same time and leaves no difference of tidal phase. The tides from Florida to Nova Scotia are the case. The northerly water may form a progression of tidal phases oriented north in the North Atlantic. Furthermore, a large body of northeasterly water would enter the strait of Gibraltar and cross the Celtic Sea, from where it continues to run into the English Channel and other related regions, a series of progressive tides along the shores of these regions are determined, the tides around England shores are the case. The southerly water also may form a progression of tidal phases oriented south in the South Atlantic. With the passage of time, the Atlantic ocean basin begin to fall from east to west, water slowly restores. On the whole, the falling of the middle of the Atlantic basin would lead water to flow in. This may give rise to a progression of tidal phases towards north at South Atlantic and towards south at North Atlantic. However, tide observations appear to show the progression of tidal phases towards south is not apparent as that towards north. This could ascribe to the influences of the trumpet-shaped North Atlantic and of the trumpet-shaped South Atlantic. The width of North Atlantic reaches 6400 km at 22° N and 3500 km at 52° N, similarly, the width of South Atlantic reaches 3800 km at 5° S and 5500 km at 33° S. The southerly water at North Atlantic and at South Atlantic may be decompressed to minify as the channel becomes wide. In contrast, the northerly water at South Atlantic and at North Atlantic would be narrowed to amplify as the channel becomes narrow.

Newton in his book *Mathematical Principles of Natural Philosophy* described a tide (Proposition XXIV. Theorem XIX, translated by Andrew Motte): "*An example of all which Dr. Halley has given us, from the observations of seamen in the port of Batsham, in the Kindom of Tunquin (presently Viet Nam), in the latitude of $25^{o}50'$ north. In that port, on the day which follows after the passage of the moon over the equator, the waters stagnate: when the moon declines to the north, they begin to flow and ebb, not twice, as in other ports, but once only every day: and the flood happens at the setting, and the greatest ebb at the rising of the moon. This tide increases with the declination of the moon till the 7th or 8th day; then for the 7 or 8 days following it decreases at the same rate as it had increased before, and ceases when the moon changes its declination, crossing over the equator to south. After which the flood is immediately changes into an ebb; and thenceforth the ebb happens at the setting and the flood at the rising of the moon; till the moon, again passing the equator, changes its declination.*" Similar tide also appears in the Australian Gulf of Carpentaria. The tide at this location reduce to zero when the Moon's declination is zero, increasing to their largest values

when the Moon is at its greatest declination, either north or south of the equator. This tide is presently called diurnal tide. Here we demonstrate how this tide forms under the frame of the rotating deformed solid Earth. As shown in Figure 8, when the Moon declines to the north, as the elongation of solid Earth is always in the Earth-Moon line and tracks from east to west, the part of the northern hemisphere of solid Earth is raised at the Moon's rising, this leads water to flow out, the water level at the location (marked with Z) falls naturally. With the passage of time, the part of the southern hemisphere of solid Earth is raised at the Moon's setting, this leads water to flow out, at least, there is a water transferring towards the north, the water level at the location rises; When the Moon declines to the south, the part of the southern hemisphere of solid Earth is raised at the Moon's rising, this leads water to flow out, at least, there is a water transferring towards the north, the water level at the location rises. With the passage of time, the part of the northern hemisphere of solid Earth is raised at the Moon's setting, this leads water to flow out, the water level at the location falls. This process eventually gives the location one high water and one low water per day. When the Moon is about the equator, the water transferring between the northern and southern hemispheres is slight, the water at the location become nearly motionless.
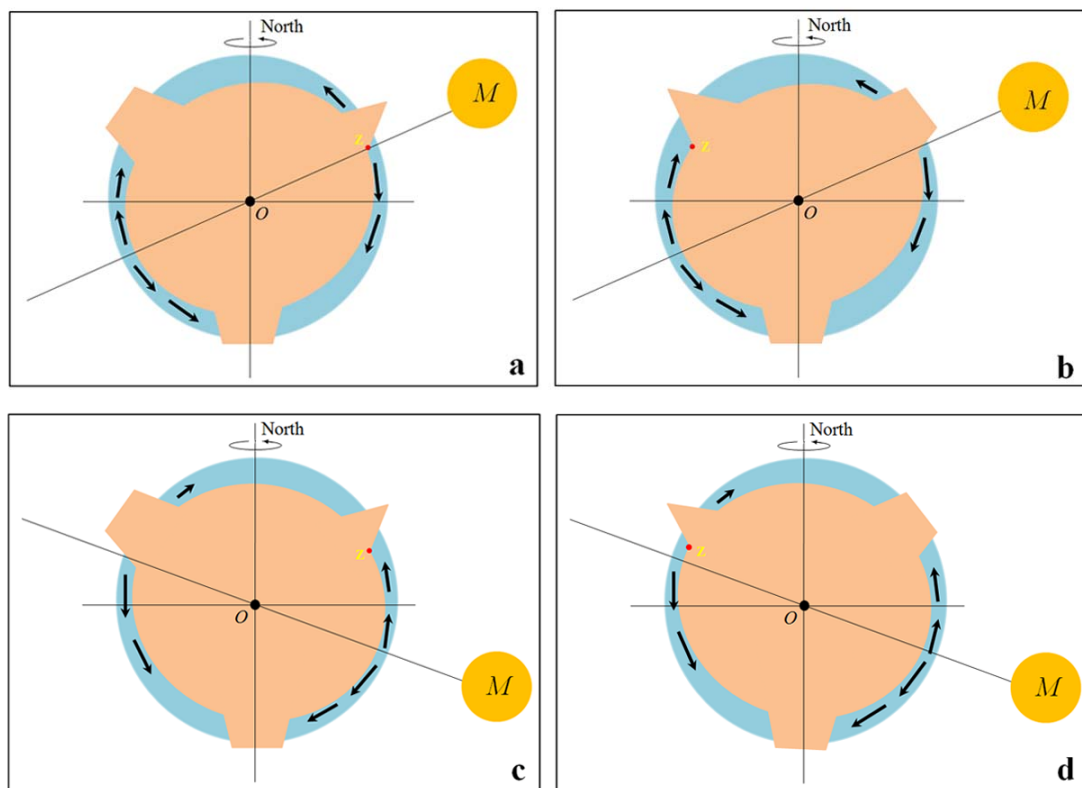
Figure 8: Modelling the formation of diurnal tide in Batsham and Karumba (red). From **a**(**b**) to **c**(**d**) the Moon transfers from north to south. From **a**(**c**) to **b**(**d**), the Earth rotates 180°. Please note, the deformation of solid Earth is highly exaggerated. *M* represents the Moon. Black arrows in each diagram denote water transferring caused by the elongation. Note the deformation of solid Earth is highly exaggerated.

Galileo in his *Dialogue Concerning the Two Chief World Systems* described the tides of the Mediterranean (translated by Stillman Drake): "*three varieties of these hourly changes are observed: in some places the waters rise a fall without making any forward motions; in others, without rising or falling they move now toward the east and again run back toward the west; and in still others, the height and the course both vary. This occurs here in Venice, where the waters rise in entering and fall in departing. ... ..., elsewhere the water runs to and fro in its central parts without changing height, as happens notably in the Straits of Messina between Scylla and Charybdis, where the currents are very swift because of the narrowness of the*

channel. But in the open Mediterranean and around its islands, such as the Balearics, Corsica, Sardinia, Elba, Sicily (on the African side), Malta, Crete, etc., the alterations of height are very small but the currents are quite noticeable, especially where the sea is restrained between islands, or between these and the continent." The Mediterranean is like a perfect vessel of water. Under the frame of the deformation of solid Earth, the two ends of this vessel regularly rise and fall as the Earth spins, this yields water transferring between the two ends, refer to Figure 5, the greatest alternation of water level occurs at the two ends, whereas the smallest occurs in the open area. The travelling water, if constrained by the straits, would form swift currents.

Some believe that the established tidal theories are competent for tide prediction. This is not the fact. It's long known that tide prediction is made from tide observation. Tidal variations (the height and time of high and low water) are observed continuously at many locations throughout the globe. When tide records become available, we may use computers to analyze the data to identify constituents of the complex wave. This works out the wave heights and time lags (in relation to the Moon's orbital movement or other motions) of each of the many different tidal constituents. Once the timing, periodicity, and the amplitude of each constituent are obtained for a particular location, a simple addition of these constituents gives the tidal height at the future time. To some extent, the success of tide prediction is a result of the development of computer technology and the collection of tide observation.

References
1. Pugh D. T. (1987). Tides, Surges and Mean Sea-Level; a handbook for engineers and scientists. JOHN WILEY & SONS.
2. Cartwright D. E. (1999). Tides: A Scientific History. Cambridge University Press.
3. Deacon, M. (1971). Scientists and the Sea, 1650-1900. London: Academic Press.
4. Pugh, D. T., and P. L. Woodworth (2014). Sea-Level Science: Understanding Tides, Surges Tsunamis and Mean Sea-Level Changes. Cambridge Univ. Press, Cambridge, U. K.
5. Lambeck, K. (1988). Geophysical Geodesy. Clarendon Press, Oxford, U. K.
6. Munk, W. (1997). Once again: Once again-Tidal friction. Progr. Oceanogr., 40, 7-35.
7. Vlasenko, V., N. Stashchuk, and K. Hutter (2005). Baroclinic Tides: Theoretical Modeling and Observational Evidence. Cambridge Univ. Press, Cambridge, U. K.
8. Pekeris, C. L., and Y. Accad (1969). Solution of Laplace's equations for the M_2 tide in the world oceans. Philos. Trans. R. Soc. A, A265, 413-436.
9. Schwiderski, E. W. (1979). Global ocean tides: Part II. The semidiurnal principal lunar tide 84 (M_2). Atlas of Tidal Charts and Maps, NSWC Tech. Rep. 79-414.
10. Fu, L.-L., and A. Cazenave (Eds.) (2001). Satellite Altimetry and Earth Sciences: A Handbook of Techniques and Applications. Academic Press, San Diego, Calif.
11. Visser, P. N. A. M., N. Sneeuw, T. Reubelt, M. Losch, and T. van Dam (2010). Space-borne gravimetric satellite constellation and ocean tides: Aliasing effects. Geophys. J. Int., 181, 789-805.
12. Stammer, D., et al. (2014). Accuracy assessment of global barotropic ocean tide models. Rev. Geophys., 52, 243-282,
13. Robert, H. S. (2008). Introduction To Physical Oceanography. Texas A& M University.
14. Fowler, C. M. R. (2004). The Solid Earth: An Introduction to Global Geophysics(2nd Education). Cambridge University Press.

15. National Research Council (U.S.). Panel on Solid Earth Problems (1964). Solid-earth Geophysics: Survey and Outlook. National Academies.
16. Council, National Research. (1993). Solid-earth sciences and society. Washington, D.C., National Academy Press.
17. Jordan, T. H. (1979). Structural Geology of the Earth's Interior. Proceedings of the National Academy of Sciences. 76 (9): 4192-4200.
18. Wootton, A. (2006). Earth's Inner Fort Knox. Discover. 27 (9): 18.
19. Stixrude, L., Cohen, R. E. (1995). High-Pressure Elasticity of Iron and Anisotropy of Earth's Inner Core. Science. 267:1972-75.
20. Ozawa, H., al., et. (2011). Phase Transition of FeO and Stratification in Earth's Outer Core. Science. 334(6057): 792-794.
21. Herndon, J. M. (1980). The chemical composition of the interior shells of the Earth. Proc. R. Soc. Lond. A372(1748): 149-154.
22. Herndon, J. M. (2005). Scientific basis of knowledge on Earth's composition. Current Science. 88(7): 1034-1037.
23. Birch, F. (1964). Density and Composition of Mantle and Core. Journal of Geophysical Research Atmospheres. 69(20):4377-4388.
24. Monnereau, M., Calvet, M., Margerin, L., Souriau, A. (2010). Lopsided Growth of Earth's Inner Core. Science. 328 (5981): 1014-1017.
25. Stixrude, L., Cohen, R. E. (1995). High-Pressure Elasticity of Iron and Anisotropy of Earth's Inner Core. Science. 267 (5206): 1972-1975.
26. Schettino, A. (2014). Quantitative Plate Tectonics. pp 245-255. Springer International Publishing Switzerland.
27. Heiskanen, W. A. (1962). Is the Earth a triaxial ellipsoid? Journal of Geophysical Research. 67 (1): 321-327.
28. Burša, M. (1993). Parameters of the Earth's tri-axial level ellipsoid. Studia Geophysica et Geodaetica. 37(1): 1-13.
29. Kopal, Z. (1969). Dynamics of the Earth-Moon System. Springer Netherlands. pp 55-68
30. Schureman, P. (1976). Manual of Harmonic Analysis and Prediction of Tides. United States Government Printing Office, Washington, 317 pp.
31. Smart, W. M. (1940). Spherical Astronomy. Cambridge University Press, 430 pp.
32. Doodson, A. T. and Warburg, H. D. (1941). Admiralty Manual of Tides. London: HMSO, 270 pp.
33. Kaula, W. M. (1968). Introduction to Planetary Physics: the Terrestrial Planets. London: John Wiley,-490pp.
34. Roy, A. E. (1978). Orbital Motion. Bristol: Adam Hilger, 489 pp.
35. Pidwirny, M. (2006). Introduction to the Oceans. Fundamentals of Physical Geography, 2nd Edition.
36. Wieczorek, M., et al. (2006). The constitution and structure of the lunar interior. Reviews in Mineralogy and Geochemistry. 60(1): 221-364.
37. Luzum, B., et al. (2011). The IAU 2009 system of astronomical constants: The report of the IAU working group on numerical standards for Fundamental Astronomy. Celestial Mechanics and Dynamical Astronomy. 110(4): 293-304.
38. Various (2000). David R. Lide, ed. Handbook of Chemistry and Physics (81st ed.).
39. Simon, J. L., et al. (1994). Numerical expressions for precession formulae and mean elements for the Moon and planets. Astronomy and Astrophysics. 282 (2): 663-683.
40. Williams, D. R. (2013). Sun Fact Sheet. NASA Goddard Space Flight Center.
41. Stevens, C. L., et al. (2012). Tidal Stream Energy Extraction in a Large Deep Strait: the Karori Rip, Cook Strait. Continental Shelf Research. 33: 100-109.
42. Bowman, M.J., et al. (1983). Circulation and mixing in greater Cook Strait, New Zealand. Oceanologica Acta. 6(4): 383-391.